Open Access

Advances in Environmental and Engineering Research

LIDSEN Publishing Inc.

Original Research

Electrochemical Oxidation of Perfluorooctanesulfonate by Magnéli Phase Ti_4O_7 Electrode in the Presence of Trichloroethylene

Peizeng Yang [1, 2], Yaye Wang [1], Junhe Lu [2, *], Viktor Tishchenko [1], Qingguo Huang [1, *]

1. Department of Crop and Soil Sciences, University of Georgia, Griffin, GA 30223, USA; E-Mails: yangpeizengnjau@yeah.net; yw53153@uga.edu; viktort@uga.edu; qhuang@uga.edu
2. Department of Environmental Science and Engineering, Nanjing Agricultural University, Nanjing, 210095, China; E-Mails: yangpeizengnjau@yeah.net; jhlu@njau.edu.cn

* **Correspondence:** Junhe Lu and Qingguo Huang; E-Mails: jhlu@njau.edu.cn; qhuang@uga.edu

Academic Editor: Zed Rengel

Special Issue: Remediation of PFAS (Per- and Polyfluoroalkyl Substances) Contamination

Adv Environ Eng Res
2020, volume 1, issue 4
doi:10.21926/aeer.2004006

Received: November 02, 2020
Accepted: December 17, 2020
Published: December 29, 2020

Abstract

This study examined the degradation of perfluorooctanesulfonate (PFOS) in electrochemical oxidation (EO) processes in the presence of trichloroethylene (TCE). The EO experiment was performed in a gas-tight reactor using Magnéli phase titanium suboxide (Ti_4O_7) as the anode. The experimental data demonstrated that 75% of PFOS (2 µM) was degraded at 10 mA/cm^2 current density in 30 min without TCE present in the solution, while the presence of 76 µM TCE apparently inhibited the degradation of PFOS, reducing its removal down to 53%. Defluorination ratio suggested that PFOS was significantly mineralized upon EO treatment, and it appeared to be not influenced by the presence of TCE. The respective pseudo-first order rate constants (k_{obs}) of PFOS removal were 0.0471 and 0.0254 min^{-1} in the absence and presence of TCE. The degradation rates of both PFOS and TCE increased with current density rising from 2.5 to 20 mA/cm^2. In the presence of TCE, chloride, chlorate, and perchlorate were formed that accounted for 79.7 %, 5.53%, and 1.51% of the total chlorine at 60 min. This work illustrates the promise of the Magnéli phase Ti_4O_7 electrode based electrochemical oxidation

technology for degrading per- and polyfluoroalkyl substances (PFASs) and co-contaminants in groundwaters.

Keywords
Perfluorooctanesulfonate; trichloroethylene; electrochemical oxidation; titanium suboxide electrode

1. Introduction

Per- and polyfluoroalkyl substances (PFASs), including perfluorooctanoate (PFOA) and perfluorooctanesulfonate (PFOS), are a group of synthetic chemicals for numerous industrial and consumer applications such as semiconductor, medical devices, aviation, and metal plating since 1950s [1-4]. Studies have found that PFASs are widely presented in surface waters, groundwaters, and effluents of wastewater treatment plants (WWTPs) with concentrations ranging from 1 ng/L to 50 μg/L [5]. PFASs are relatively mobile and extremely stable in the environment. Once released into the natural environment, they are readily transported with water flow contaminating larger areas [6-8]. In particular, some long-chain PFASs can cause liver malfunction, hypothyroidism, high cholesterol, adverse neurobehavioral effects and tumors in multiple organ systems [9]. Hence, the global distribution, environmental persistence, and potential toxicity of PFASs have raised great concerns to both the public and regulatory agencies [10]. PFASs have been added to the list of persistent organic pollutants (POPs) by Stockholm Convention [11]. The United Sates Environmental Protection Agency (USEPA) established a health advisory level (HAL) for PFOA and PFOS in drinking water at 70 ng/L [12].

Due to their extreme chemical and thermal stability, PFASs are highly resistant to conventional treatment technologies and even advanced oxidation processes [13-15]. Recent studies showed that electrochemical oxidation (EO) could be a promising technology to address PFASs contamination [16-26]. Electrochemical degradation of PFASs at ambient conditions (i.e., room temperature and atmospheric pressure) without adding reagents have been reported by using boron-doped diamond (BDD) anodes or Sb and Pb doped titanium-based anodes [16-22]. Direct anodic oxidation and indirect oxidation by hydroxyl radicals (HO•) were found to be the main mechanisms of PFASs degradation. More recently, we found that Magnéli phase titanium suboxide ceramic showed a great efficiency on the degradation of PFASs [23-27]. A complete removal of PFOA and PFOS (both at 2 μM) was achieved in a batch system in 60 min at a current density of 5 mA/cm^2 [25]. The removal efficiency of PFOS in reactive electrochemical membrane (REM) systems with a porous Magnéli phase titanium suboxide ceramic membrane serving simultaneously as the anode and the membrane was much greater than that of the batch system under the same anodic potential. Nearly complete removal of PFOS (2 μM) was achieved in such a REM system at the current density of 4 mA/cm^2 [26].

Magnéli phase titanium suboxide ceramic is considered as an ideal anode material for electrochemical applications due to its cost-effectiveness, durability, high conductivity, and environmentally friendly natures [28]. These materials comprise a series of distinct compounds having a generic formula (Ti_nO_{2n-1}, $3< n <10$). Among them, Ti_4O_7 exhibits the greatest conductivity

[29]. It has a wide electrochemical window with regard to water oxidation and reduction [29], thus can direct electrochemical treatment of pollutants in water over a wide range of redox potential. Studies have reported that Ti_4O_7 behaves as typical "non-active" electrodes and thus produces HO• via water oxidation, and is also active for direct electron transfer reactions which thus promotes PFOA and PFOS electron transfer and subsequent complete mineralization [27].

Trichloroethylene (TCE) is a high volatile and toxic chemical used as an industrial solvent, household cleaner, and metal degreaser. It has widespread occurrence in groundwaters due to the leakage from underground storage tanks and improper treatment in landfills [30-32]. It was reported that firefighter training exercises often released fire-fighting foams which contained PFASs, as well as fuels into the environment [10, 33]. Chlorinated solvents such as TCE were ignited as the flammable component in these training exercises [34], thus, the infiltrated water was likely to contain PFASs and TCE concurrently [34]. Therefore, it requires careful examination of their effects on each other during the EO process. There have been some reports on electrochemical treatment of TCE on BDD anode. It showed that TCE could be efficiently removed via direct electron transfer and indirect oxidation by HO• [35, 36]. The degradation of TCE on anode involved a series of reactions of TCE dechlorination and chloride (Cl^-) formation. Cl^- can be converted into reactive chlorine species on the anode and further to chlorate (ClO_3^-) [35]. The degradation of TCE on BDD anode is relatively clear, but its transformation on Ti_4O_7 anode and its impact on electrochemical degradation of PFASs are still unknown.

In this study, a gas-tight reactor was developed to investigate the electrochemical degradation of PFOS in the presence of TCE on a Magnéli phase Ti_4O_7 anode. The reaction kinetics of PFOS and TCE in this process were both examined, and the formation of Cl^-, ClO_3^-, and ClO_4^- were monitored. This work is relevant in assessing the feasibility of electrochemical degradation of PFASs and co-contaminants on Ti_4O_7 anode in groundwaters.

2. Materials and Methods

2.1 Chemicals and Materials

All chemicals were of the purest available quality. Perfluorooctanesulfonic acid (PFOS, 98%) was purchased from Indofine Chemical Company, Inc. (Hillsborough, NJ). Sodium perfluoro-1-[^{13}C8]-octanesulfonate (M8PFOS) was obtained from Wellington Laboratories (Guelph, Ontario, Canada). Trichloroethylene (TCE, > 98%), sodium sulfate (Na_2SO_4), sodium chloride (NaCl), sodium chlorate ($NaClO_3$), and sodium perchlorate ($NaClO_4$) were purchased from Sigma-Aldrich (St. Louis, MO, USA). HPLC grade methanol, methyl tert-butyl ether (MTBE), ammonium acetate, and ethyl acetate were purchased from Fisher (Waltham, MA, USA). Except for TCE, other solutions were prepared in ultrapure water (≥ 18.2 MΩ•cm) produced by a Barnstead Nanopure water purification system. TCE stock solution was prepared in ultrapure water with 0.1% methanol. PFOS and TCE working solution was made by diluting appropriate stock solution in ultrapure water.

Plate Ti_4O_7 ceramic electrode was synthesized through a high temperature sintering process as described in a prior study [23]. Detailed procedure can be found in the supporting information (SI). The characterization of Ti_4O_7 anode used in this study has been reported in our earlier study [27]. Magnéli phase Ti_4O_7 was confirmed as the dominant composition of the electrode material by XRD characterization (Figure S1a and S1b). They have interconnected micropores with diameters smaller

than 10 µm by SEM analysis (Figure S1c) and a porosity of 21.6%, a median pore diameter of 3.6 µm (based on volume) or 2.8 µm (based on area), and an average pore diameter of 2.6 µm by mercury intrusion analysis (Figure S1d).

2.2 Reaction Setup

All experiments were performed at room temperature (25 °C) in a gas-tight EO reactor. A picture and scheme of the gas-tight EO reactor are provided in Figure 1. The electrolysis cell was placed inside a gas tight cylindrical container along with an Erlenmeyer flask containing 20 mL ethyl acetate that served as a trap to collect volatile products. Two small holes were made on the lid and fitted with rubber caps for sampling. A controllable DC power source (Electro Industries Inc., Monticello, MN, USA) was connected with the electrolytic cell through copper wires and alligator clamps. Electrochemical oxidation experiments were conducted in the electrolytic cell (10 cm × 5 cm × 2.5 cm) with a Ti_4O_7 ceramic plate (10 cm × 5 cm) as the anode and two 304-stainless steel plates of the same size as the cathode. The electrolytic cell was undivided, and the anode was placed between two cathodes in parallel with an inter-electrode distance of 2.5 cm.

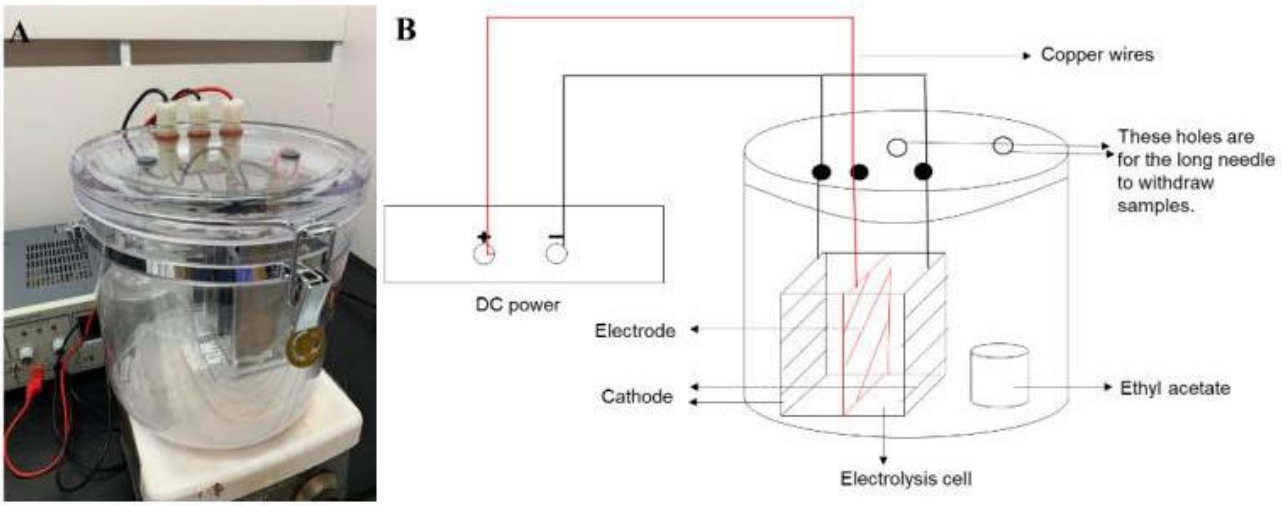

Figure 1 Picture and scheme of Gas-tight EO reactor.

In each treatment, 200 mL solution of 2 µM PFOS (1 mg/L), 76 µM TCE (10 mg/L), and 100 mM Na_2SO_4 as background electrolyte was placed in the electrolytic cell with continuous stirring. Different current densities (2.5, 5, 7.5, 10, 15, and 20 mA/cm^2) were applied to the electrolytic cell based on the electrode area submerged in the solution (75 cm^2) using the DC power source. The anodic potential was monitored using a CHI 660E electrochemical workstation (CH Instruments Inc., Austin, TX, USA) with silver chloride reference electrode placed in the cell. All anodic potentials are reported against standard hydrogen electrode (SHE). When current density was at or below 20 mA/cm^2, the passivation of anodic polarization was verified to be negligible in our previous study [27]. Controls with sole PFOS or TCE were prepared concurrently. At pre-set time intervals, the power source was paused with the solution continuously stirred to ensure homogeneity. Then, 0.5 mL of the solution was sampled from the electrolytic cell. Among them, 0.4 mL solution was transferred to a 1.5 mL centrifuge tube with 0.4 mL methanol containing 0.1 µM of M8PFOS as the

internal standard. Samples were further centrifuged at 7500 rpm for 5 min and passed through 0.22 µM nylon-based syringe filters, stored at 4 °C for PFOS analysis. The rest sample solution was mixed with 0.9 mL ultrapure water for detecting Cl^-, ClO_3^-, and ClO_4^-. Another 1 mL of the solution was sampled and extracted with 3 mL MTBE according to the standard USEPA method 551.1 for TCE analysis [37]. Additionally, 0.5 mL of the ethyl acetate in the trap solution was sampled for TCE and other volatile substances analysis.

2.3 Mass Analysis

PFOS was analyzed using a Waters Acquity UPLC system coupled with Xevo TQD tandem mass spectrometry (UPLC/MS/MS) with electrospray ionization (ESI) source (Milford, MA, USA). MS was operated at negative ESI. A Waters Acquity UPLC BEH C18 column (50 mm × 2.1 mm, i.d., 1.7 µm) was used for separation. PFOS and its isotope labeled standard were identified using multiple reaction monitoring (MRM) mode based on the transition patterns: *m/z* = 499 > 80 for PFOS and *m/z* = 507 > 99 for M8PFOS. Quantification was achieved by the ratio of the MRM signal of the chemical to that of the internal standard in reference to a five-point calibration curve. ClO_3^- and ClO_4^- were also analyzed using the UPLC/MS/MS at negative ESI. They were analyzed at MRM mode based on the transition *m/z* = 83 > 67 and *m/z* = 99 > 83 for ClO_3^- and ClO_4^-, respectively. The concentrations of ClO_3^- and ClO_4^- were quantified with an external calibration curve. More detailed instrumental parameters setup can be found in the SI.

TCE in the reaction solution was extracted with MTBE according to the standard USEPA method 551.1 and analyzed using an Agilent 7890A gas chromatography coupled with 5975B mass spectrometry (GC/MS) and a DB-5MS chromatographic column (30 m × 0.25 mm, i.d., 0.25 µm) (Santa Clara, CA, USA). The temperature program was set as follows: initial temperature of 35 °C held for 5 min, then increased at a rate of 10 °C/min to 260 °C, and held for additional 2 min. The temperature of the injector and detector were 200 °C and 260 °C, respectively. Five calibration standards in MTBE, bracketing the analyte concentration range expected in the samples, were analyzed together with each set of samples. TCE in ethyl acetate was also analyzed using GC/MS as above, along with external calibration samples prepared in ethyl acetate.

2.4 Fluoride Analytical Method

The fluoride (F^-) in treated PFOS samples was quantified using a F^- selective electrode (Thermo Scientific™ Orion™) by a standard addition method [38]. Details can be found in the SI. The defluorination ratio (F_r) was calculated according to Eq. (1):

$$F_r = \frac{C_{F,t} - C_{F,0}}{(C_0 - C_t) \times 17} \times 100\% \quad (1)$$

Where $C_{F,t}$ and $C_{F,0}$ are the concentrations of F^- in treatment solution at time t and 0, respectively; C_0 and C_t are the concentrations of PFOS at time 0 and t, respectively, and the factor 17 corresponds to the number of fluorine atoms in a PFOS molecule.

2.5 Ion Chromatography Analysis

Cl^- was analyzed using a Shimadzu ion chromatography (Shimadzu Corp., Kyoto, Japan) coupled with a Shodex IC SI-52 4E column (250 mm × 4 mm, i.d., 5 μm). The column temperature and suppressor current were maintained at 40 °C and 40 mA, respectively. The mobile phase of 3.6 mM sodium carbonate was run at a flow rate of 0.8 mL/min for total 30 min. The concentration of Cl^- was quantified with an external calibration curve.

3. Results and Discussion

3.1 Degradation of PFOS in the Presence of TCE

Both linear and branched PFOS (L-PFOS and B-PFOS) were contained in the tested PFOS sample, and the ratio between them was approximately 33:2 (L-PFOS/B-PFOS) based on their responses in MRM as mentioned in our previous study [25]. L-PFOS and B-PFOS were monitored separately in the experiments. Results showed that the degradation behaviors of L-PFOS and B-PFOS were similar (data not shown), and thus only L-PFOS data were reported in the following discussion. PFOS (2 μM) was rapidly removed in electrochemical oxidation processes with Ti_4O_7 anode (Figure 2a). The removal of PFOS was apparently inhibited in the presence of 76 μM TCE, with only 53% removal in 30 min compared to 75% in the absence of TCE at identical conditions. In both cases, the removal of PFOS can be well fitted by pseudo-first order kinetic model ($R^2 > 0.91$). The pseudo-first order rate constants (k_{obs}) of PFOS removal were 0.0471 and 0.0254 min^{-1} without and with TCE, respectively. It was proposed that PFOS can be oxidized at anode through direct electron transfer and then followed by reactions with HO• at anode and/or adsorbed hydrogen at cathode to release fluoride [26, 39]. Hydroxyl radicals can be *in situ* generated from water electrolysis when the anode potential is greater than 2.38 V (vs. SHE) [23]. The presence of TCE may inhibit the removal of PFOS by competing for electron transfer sites and HO•.

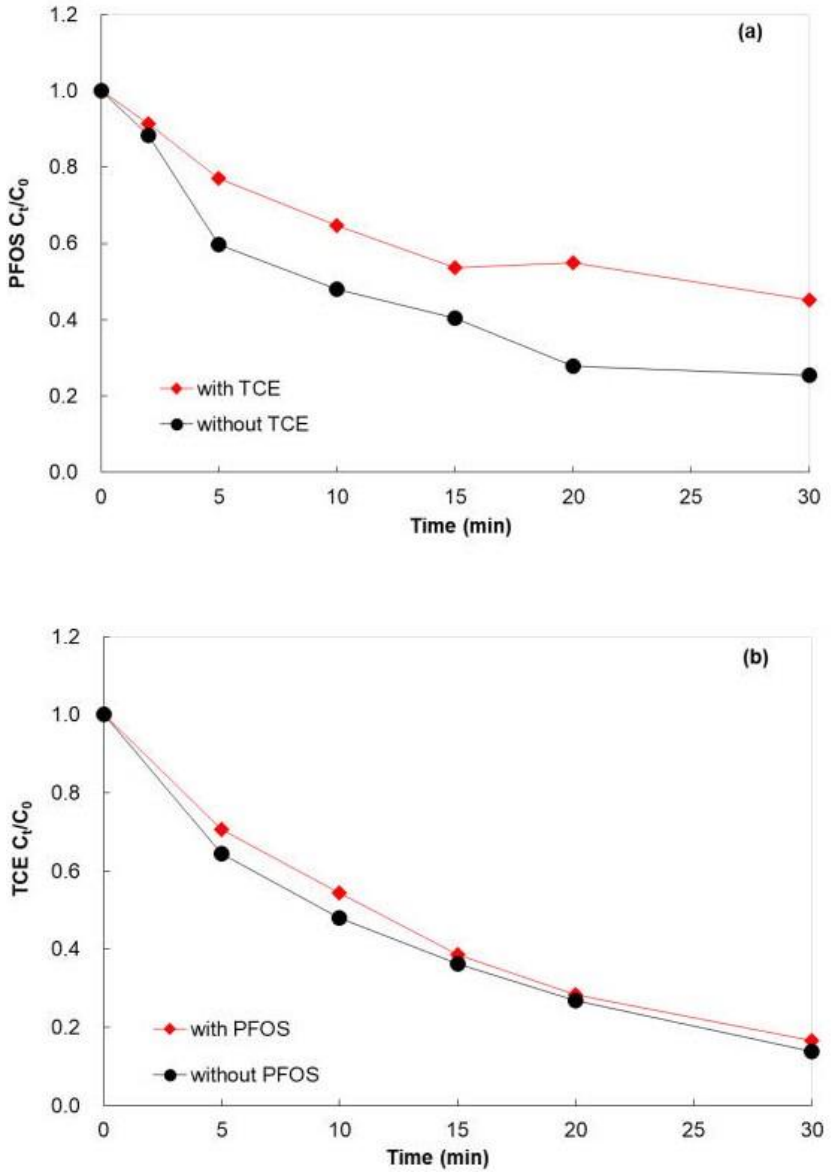

Figure 2 Removal of (a) PFOS and (b) TCE in the EO process with Ti_4O_7 anode. Experimental condition: PFOS 2 µM (1 mg/L), TCE 76 µM (10 mg/L), Na_2SO_4 100 mM, reaction volume 200 mL, current density 10 mA/cm^2.

Removal of TCE in EO processes with Ti_4O_7 anode was also investigated (Figure 2b). Since TCE is volatile, its loss due to evaporation was collected by an ethyl acetate trap solution placed alongside the electrolytic cell in the gas-tight container. Little TCE evaporation occurred during the reaction. After 60 min, only 2.69% of TCE was detected in ethyl acetate. However, 13.45% of TCE was left in the reaction solution at that time (Figure S2). Data suggested that most of TCE was degraded rather than escaped to atmosphere. Regardless of the TCE evaporative loss, the k_{obs} value of TCE removal would be equivalent to 0.0621 min^{-1} ($R^2 > 0.99$), indicating faster TCE degradation compared to PFOS. Noteworthy, the presence of PFOS slightly affected the removal of TCE. A removal of 86.2% was achieved in 30 min in the absence of PFOS compared to 83.5% when PFOS was present (Figure 2b). The k_{obs} value of TCE removal in the presence of PFOS was 0.0601 min^{-1} ($R^2 > 0.99$).

3.2 Influence of Current Density

Electrochemical oxidation of PFOS in the presence of TCE was further examined under various current densities. Results showed that an increase in current density facilitated the degradation of both PFOS and TCE (Figure S3). The removal of PFOS in 30 min increased from 41.65% to 92.62%, corresponding to the k_{obs} of PFOS increasing from 0.0162 to 0.0786 min^{-1}, when the current density raised from 2.5 to 20 mA/cm^2. The removal of TCE increased from 66.54% to 100%, corresponding to the k_{obs} of TCE increasing from 0.0382 to 0.1263 min^{-1}. Pseudo-first order rate constants of both PFOS and TCE degradation at different current densities are presented in Table 1. Surface area normalized rate constants (k_{SA}) of PFOS and TCE were calculated according to Eq. (2):

$$k_{SA} = k_{obs}\frac{V}{A} \quad (2)$$

where V is the total volume of the reaction solution (m^3); A is the anode geometry surface area in solution (m^2).

Table 1 Pseudo-first order kinetic constants of electrochemical degradation of PFOS and TCE with Ti_4O_7 anode.

Current density (mA/cm^2)	Anode potential (V)	k_{obs} of TCE (min^{-1})	k_{obs} of PFOS (min^{-1})	k_{SA} of TCE (m/s)	k_{SA} of PFOS (m/s)
2.5	3.45	0.0382 ± 0.0018	0.0162 ± 0.0018	$1.70\times10^{-5} \pm 5.22\times10^{-7}$	$7.20\times10^{-6} \pm 7.80\times10^{-7}$
5.0	3.72	0.0411 ± 0.0011	0.0214 ± 0.0021	$1.83\times10^{-5} \pm 4.76\times10^{-7}$	$9.51\times10^{-6} \pm 9.16\times10^{-7}$
7.5	3.93	0.0530 ± 0.0021	0.0223 ± 0.0041	$2.36\times10^{-5} \pm 9.23\times10^{-7}$	$9.91\times10^{-6} \pm 1.80\times10^{-6}$
10.0	4.07	0.0601 ± 0.0008	0.0254 ± 0.0024	$2.67\times10^{-5} \pm 3.72\times10^{-7}$	$1.13\times10^{-5} \pm 1.08\times10^{-6}$
15.0	4.22	0.1014 ± 0.0022	0.0370 ± 0.0036	$4.51\times10^{-5} \pm 9.68\times10^{-7}$	$1.64\times10^{-5} \pm 1.62\times10^{-6}$
20.0	4.39	0.1263 ± 0.0034	0.0786 ± 0.0037	$5.61\times10^{-5} \pm 1.39\times10^{-6}$	$3.49\times10^{-5} \pm 1.64\times10^{-6}$

The $\pm$ bracket represents 95% confidence level (CL)

Since V and A of the solution were constant for the same reactor, Eq. (2) means k_{SA} values of PFOS and TCE were proportional to the respective k_{obs} values.

The anode potential at different current densities was also monitored. The value increased from 3.45 to 4.39 V when the current density increased from 2.5 to 20 mA/cm^2 (Table 1). The relationship between the anode potential and k_{SA} is shown in Figure 3. The k_{SA} of PFOS raised from 7.20×10^{-6} to 3.49×10^{-5} m/s and the k_{SA} of TCE raised from 1.70×10^{-5} to 5.61×10^{-5} m/s with increased anode potential. At the same anode potential, the k_{SA} of TCE was much greater than that of PFOS which suggested that the degradation of TCE was easier than that of PFOS.

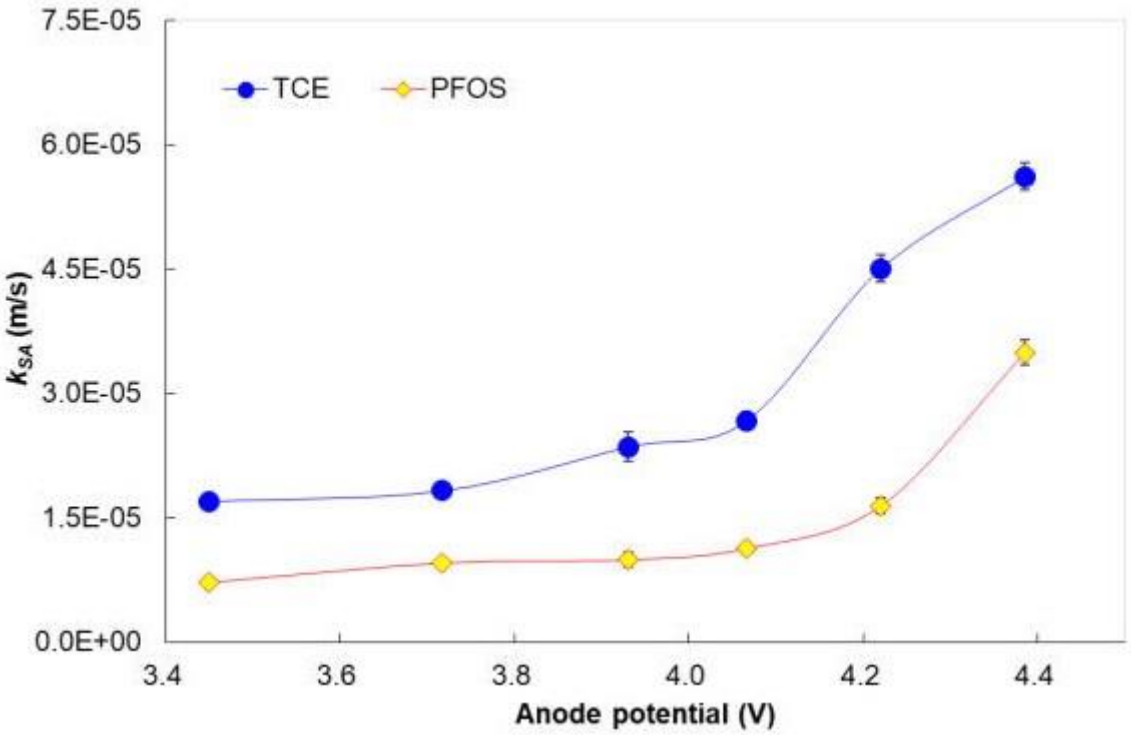

Figure 3 Relationship of surface area normalized rate constants (k_{SA}) of PFOS and TCE and anode potential. Experimental condition: PFOS 2 µM (1 mg/L), TCE 76 µM (10 mg/L), Na_2SO_4 100 mM, reaction volume 200 mL, current density 2.5, 5, 7.5, 10, 15, and 20 mA/cm^2.

The limiting current density can be analyzed according to the limiting current technology proposed in previous studies [27, 40]. The limiting current density (5.3 mA/cm^2) was determined experimentally for 10 mM $Fe(CN)_6^{4-}$, that approximated the transition between kinetic-limited and mass transfer-limited conditions for fast reacting compounds (details can be found in the SI). EO treatment was conducted with 2 µM PFOS and 76 µM TCE under different current densities (2.5-20 mA/cm^2). The pseudo-first order rate constants were obtained by data fitting, based on which k_{SA} was calculated according to Eq. (2). Since the Ti_4O_7 electrode was porous ceramic material, the effective electro-active surface area was also calculated to be 467.37 cm^2 (details in SI) [23, 27]. Therefore, rate constants normalized by the effective electro-active surface area (k'_{SA}) were calculated for PFOS and TCE using Eq. (3):

$$k'_{SA} = k_{obs}\frac{V}{S_{active}} \quad (3)$$

where V is the treatment solution volume corresponding to the electro-active electrode surface area (m^3); S_{active} is the effective electro-active surface area (m^2).

The k'_{SA} of PFOS and TCE increased to 5.61×10^{-6} and 9.01×10^{-6} m/s, respectively, when anode potential reached to 4.39 V. The mass transfer rate constants ($k_{m,\,i}$) of PFOS and TCE were determined to be 4.11×10^{-5} and 5.94×10^{-5} m/s, respectively (details in SI) [41-43]. It can be seen that the k'_{SA} of PFOS and TCE were much lower than the $k_{m,\,i}$ of PFOS and TCE, suggesting that the EO system was kinetically limited when the current density was below 20 mA/cm^2 (anode potential 4.39 V).

3.3 Formation of Fluorinated and Chlorinated Byproducts

Short-chain perfluoroalkyl acids (PFAAs) were not detected in the aqueous solution during EO treatment of PFOS. This was in accordance with our previous findings that the formation of PFAA byproducts was minimal because they were negatively charged and could be held on the anode surface until complete mineralization [23]. Note that, F^- could be found during PFOS electrooxidation. As shown in Figure 4, fluoride release ratio after 30 min of EO treatment was 82.9% ± 1.99% and 81.0% ± 3.20%, respectively, in the presence and absence of 76 µM TCE. This suggested significant defluorination of PFOS upon EO treatment, and it appeared to be not influenced by the presence of TCE. Recent studies suggested that the reduction reactions at cathode enhanced the fluoride release of PFASs in the EO process [39]. Although the presence of TCE inhibited PFOS removal by competing for electron transfer sites and HO• at anode, the defluorination at cathode might not be inhibited and played a role.

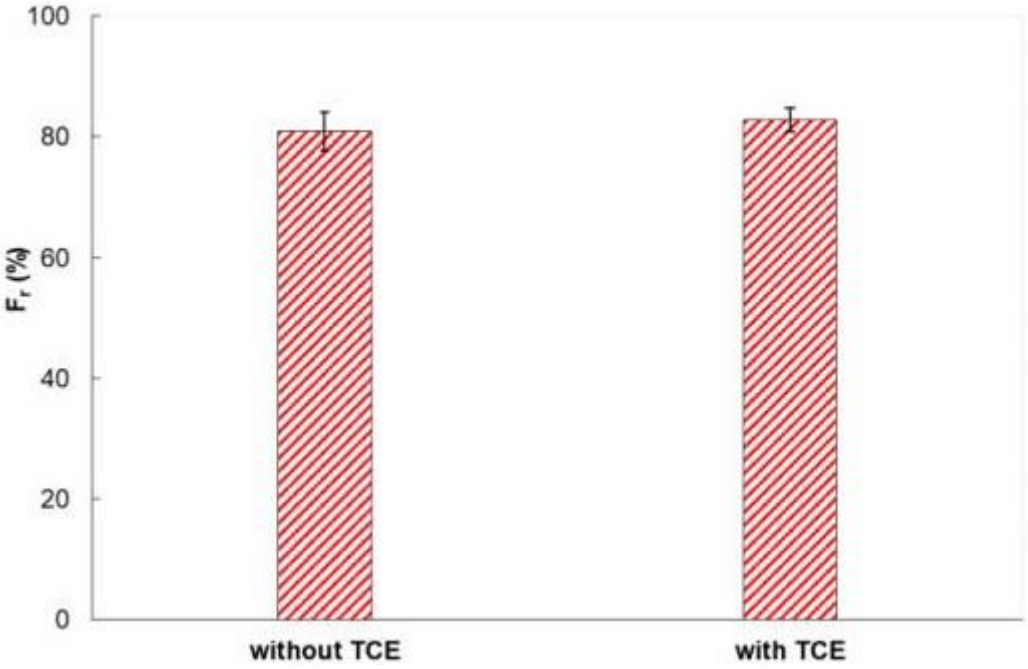

Figure 4 Floride release in the EO process with Ti_4O_7 anode. Experimental condition: PFOS 2 µM (1 mg/L), TCE 76 µM (10 mg/L), Na_2SO_4 100 mM, reaction volume 200 mL, current density 10 mA/cm^2.

It has been reported that ClO_3^- and ClO_4^- can be formed when Cl^- is present during EO processes (R1-R4) [27, 44-46]. Since a TCE molecule contains three chlorine atoms, and dechlorination occurred during its degradation, formation of Cl^-, ClO_3^-, and ClO_4^- were examined in this study. As shown in Figure 5, TCE was completely degraded in 30 min at a current density of 20 mA/cm^2. Along with its degradation, Cl^-, ClO_3^-, and ClO_4^- were formed. At 60 min, the yields of Cl^-, ClO_3^-, and ClO_4^- were 195.07, 13.53, and 3.69 µM, respectively, accounting for 79.72%, 5.53%, and 1.51% of the total chlorine. The total inorganic chlorine species and residual TCE accounted for 86.76% of the total chlorine in the reaction system at 60 min. This value, in combination with another 2.69% of vapored TCE as described above, suggested that there were parts of chlorine not detected. Dichlorination byproducts of TCE including dichloro- and chloroethylene were detected neither in the solution nor ethyl acetate. We presumed that these might be other organic chlorinated intermediates such as dichloroacetic acid from the transformation of TCE in EO processes. Noteworthy, although the concentrations of ClO_3^- and ClO_4^- were relatively low, it was well-known that they had relatively high toxicity which may cause potential risks to the environment and human, including disruption of the normal function of the thyroid gland and carcinogenic potential [47-49].

$$HO^\bullet + Cl^- \leftrightarrow ClHO^- \quad (R1)$$

$$ClHO^- + H^+ \rightarrow Cl^\bullet + H_2O \quad (R2)$$

$$HO^\bullet + Cl^\bullet \rightarrow ClO^- + H^+ \quad (R3)$$

$$ClO^- \xrightarrow{-e,+HO^\bullet,-H^+} ClO_2^- \xrightarrow{-e,+HO^\bullet,-H^+} ClO_3^- \xrightarrow{-e,+HO^\bullet,-H^+} ClO_4^- \quad (R4)$$

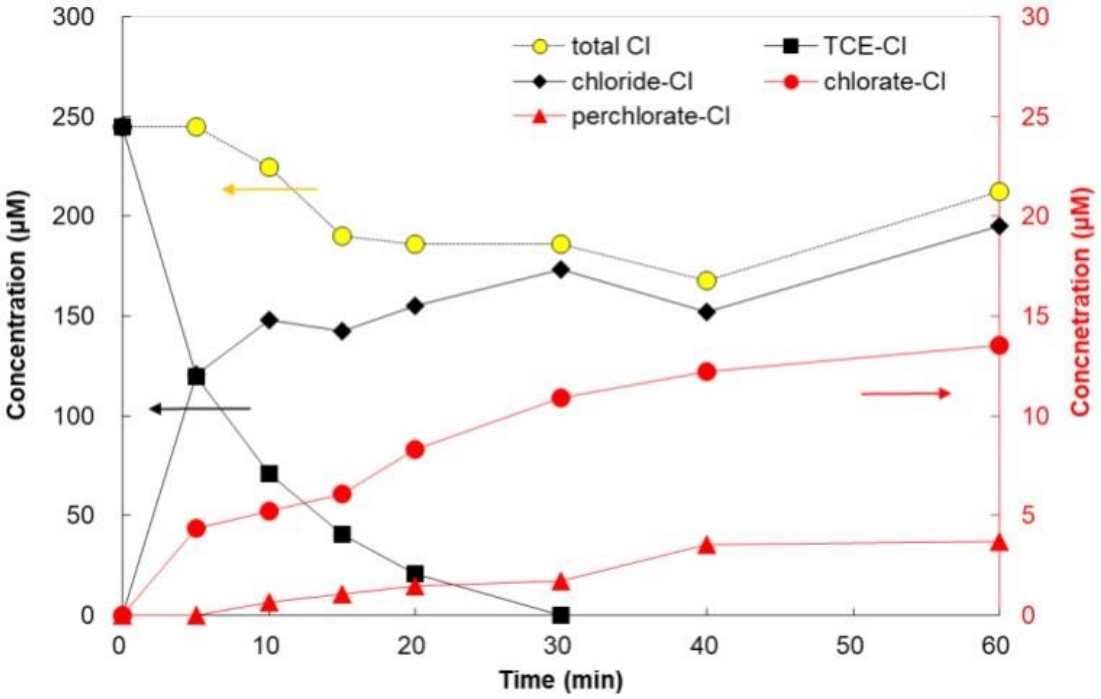

Figure 5 Formation of inorganic chlorinated byproducts during the degradation of TCE in the EO process with Ti_4O_7 anode. Experimental condition: PFOS 2 µM (1 mg/L), TCE 76 µM (10 mg/L), Na_2SO_4 100 mM, reaction volume 200 mL, current density 20 mA/cm^2.

4. Conclusions

PFOS and TCE are commonly present in groundwaters and pose continued threats to human health as human carcinogens [9, 34]. The Magnéli phase Ti_4O_7 electrode, a porous material with high conductivity and chemical stability, is able to effectively remove PFOS and TCE in water simultaneously. Results showed that the removal rates of PFOS and TCE increased with increasing current density. The presence of TCE obviously inhibited the removal of PFOS in EO processes, but the presence of PFOS only slightly suppressed the removal of TCE. Besides, defluorination ratio suggested that PFOS was significantly mineralized upon EO treatment. During this process, dechlorination of TCE occurred and Cl^- was formed. Cl^- can be further converted to undesirable ClO_3^- and ClO_4^-. Thus, the formation and control of hazardous byproducts warrants further investigation. Overall, the EO system with Ti_4O_7 anode is promising for treatment of PFOS in the presence of TCE in groundwaters.

Acknowledgments

This research was supported by in part by U.S. Department of Defense SERDP ER-2717 and ER-1320. P. Yang would like to acknowledge the support of Nanjing Agricultural University study abroad program and Postgraduate Research and Practice Innovation Program of Jiangsu Province (030-Z562015603).

Author Contributions

Peizeng Yang: Data collection and analysis, Original draft preparation. Yaye Wang: Data collection and analysis. Junhe Lu: Conceptualization, Methodology, Review and Editing. Viktor Tishchenko: Methodology, Reviewing. Qingguo Huang: Supervision, Reviewing and Editing.

Competing Interests

A patent application is pending on “Methods and Systems for Electrochemical Oxidation of Polyfluoroalkyl and Perfluoroalkyl Contaminants” (62/377,120) with QH as one of the inventors.

References

1. Kotthoff M, Muller J, Jürling H, Schlummer M, Fiedler D. Perfluoroalkyl and polyfluoroalkyl substances in consumer products. Environ Sci Pollut Res Int. 2015; 22: 14546-14559.
2. Ye F, Zushi Y, Masunaga S. Survey of perfluoroalkyl acids (PFAAs) and their precursors present in Japanese consumer products. Chemosphere. 2015; 127: 262-268.
3. Lindstrom AB, Strynar MJ, Libelo EL. Polyfluorinated compounds: Past, present, and future. Environ Sci technol. 2011; 45: 7954-7961.
4. Fiedler S, Pfister G, Schramm KW. Poly- and perfluorinated compounds in household consumer products. Toxicol Environ Chem. 2010; 92: 1801-1811.
5. Zareitalabad P, Siemens J, Hamer M, Amelung W. Perfluorooctanoic acid (PFOA) and perfluorooctanesulfonic acid (PFOS) in surface waters, sediments, soils and wastewater—A review on concentrations and distribution coefficients. Chemosphere. 2013; 91: 725-732.

6. Prevedouros K, Cousins IT, Buck RC, Korzeniowski SH. Sources, fate and transport of perfluorocarboxylates. Environ Sci Technol. 2006; 40: 32-44.
7. Houde M, De Silva AO, Muir DC, Letcher RJ. Monitoring of perfluorinated compounds in aquatic biota: An updated review. Environ Sci Technol. 2011; 45: 7962-7973.
8. Davis KL, Aucoin MD, Larsen BS, Kaiser MA, Hartten AS. Transport of ammonium perfluorooctanoate in environmental media near a fluoropolymer manufacturing facility. Chemosphere. 2007; 67: 2011-2019.
9. Blum A, Balan SA, Scheringer M, Trier X, Goldenman G, Cousins IT, et al. The madrid statement on poly- and perfluoroalkyl substances (PFASs). Environ Health Perspect. 2015; 123: A107-A111.
10. Moody CA, Field JA. Perfluorinated surfactants and the environmental implications of their use in fire-fighting foams. Environ Sci Technol. 2000; 34: 3864-3870.
11. Wang T, Wang Y, Liao C, Cai Y, Jiang G. Perspectives on the inclusion of perfluorooctane sulfonate into the Stockholm convention on persistent organic pollutants. Environ Sci Technol. 2009; 43: 5171-5175.
12. Fact Sheet: PFOA and PFOS drinking water health advisories. Washington: US Environmental Protection Agency; 2016; EPA 800-F-16-003.
13. Vecitis CD, Park H, Cheng J, Mader BT, Hoffmann MR. Treatment technologies for aqueous perfluorooctanesulfonate (PFOS) and perfluorooctanoate (PFOA). Front Environ Sci Eng CHN. 2009; 3: 129-151.
14. Trojanowicz M, Bojanowska-Czajka A, Bartosiewicz I, Kulisa K. Advanced oxidation/reduction processes treatment for aqueous perfluorooctanoate (PFOA) and perfluorooctanesulfonate (PFOS)—A review of recent advances. Chem Eng J. 2018; 336: 170-199.
15. Jin L, Zhang P, Shao T, Zhao S. Ferric ion mediated photodecomposition of aqueous perfluorooctane sulfonate (PFOS) under UV irradiation and its mechanism. J Hazard Mater. 2014; 271: 9-15.
16. Niu J, Lin H, Xu J, Wu H, Li Y. Electrochemical mineralization of perfluorocarboxylic acids (PFCAs) by ce-doped modified porous nanocrystalline PbO_2 film electrode. Environ Sci Technol. 2012; 46: 10191-10198.
17. Zhuo Q, Deng S, Yang B, Huang J, Wang B, Zhang T, et al. Degradation of perfluorinated compounds on a boron-doped diamond electrode. Electrochim Acta. 2012; 77: 17-22.
18. Lin H, Niu J, Ding S, Zhang L. Electrochemical degradation of perfluorooctanoic acid (PFOA) by Ti/SnO_2-Sb, Ti/SnO_2-Sb/PbO_2 and Ti/SnO_2-Sb/MnO_2 anodes. Water Res. 2012; 46: 2281-2289.
19. Lin H, Niu J, Xu J, Huang H, Li D, Yue Z, et al. Highly efficient and mild electrochemical mineralization of long-chain perfluorocarboxylic acids (C_9-C_{10}) by Ti/SnO_2-Sb-Ce, Ti/SnO_2-Sb/Ce-PbO_2, and Ti/BDD electrodes. Environ Sci Technol. 2013; 47: 13039-13046.
20. Carter KE, Farrell J. Oxidative destruction of perfluorooctane sulfonate using boron-doped diamond film electrodes. Environ Sci Technol. 2008; 42: 6111-6115.
21. Schaefer CE, Andaya C, Burant A, Condee CW, Urtiaga A, Strathmann TJ, et al. Electrochemical treatment of perfluorooctanoic acid and perfluorooctane sulfonate: Insights into mechanisms and application to groundwater treatment. Chem Eng J. 2017; 317: 424-432.
22. Trautmann AM, Schell H, Schmidt KR, Mangold KM, Tiehm A. Electrochemical degradation of perfluoroalkyl and polyfluoroalkyl substances (PFASs) in groundwater. Water Sci Technol. 2015; 71: 1569-1575.

23. Lin H, Niu J, Liang S, Wang C, Wang Y, Jin F, et al. Development of macroporous Magnéli phase Ti_4O_7 ceramic materials: As an efficient anode for mineralization of poly- and perfluoroalkyl substances. Chem Eng J. 2018; 354: 1058-1067.
24. Liang S, Pierce Jr RD, Lin H, Chiang SY, Huang QJ. Electrochemical oxidation of PFOA and PFOS in concentrated waste streams. Remediat J. 2018; 28: 127-134.
25. Wang Y, Shi H, Li C, Huang Q. Electrochemical degradation of perfluoroalkyl acids by titanium suboxide anodes. Environ Sci Water Res Technol. 2020; 6: 144-152.
26. Shi H, Wang Y, Li C, Pierce R, Gao S, Huang Q. Degradation of perfluorooctanesulfonate by reactive electrochemical membrane composed of magneli phase titanium suboxide. Environ Sci Technol. 2019; 53: 14528-14537.
27. Wang L, Lu J, Li L, Wang Y, Huang Q. Effects of chloride on electrochemical degradation of perfluorooctanesulfonate by Magnéli phase Ti_4O_7 and boron doped diamond anodes. Water Res. 2020; 170: 115254.
28. Walsh FC, Wills RG. The continuing development of Magnéli phase titanium sub-oxides and Ebonex® electrodes. Electrochim Acta. 2010; 55: 6342-6351.
29. Bunce NJ, Bejan D. Pollutants in water-electrochemical remediation using ebonex electrodes. Encycl Appl Alectrochem. 2014: 1629-1633.
30. Popat SC, Zhao K, Deshusses MA. Bioaugmentation of an anaerobic biotrickling filter for enhanced conversion of trichloroethene to ethene. Chem Eng J. 2012; 183: 98-103.
31. Wu X, Gu X, Lu S, Xu M, Zang X, Miao Z, et al. Degradation of trichloroethylene in aqueous solution by persulfate activated with citric acid chelated ferrous ion. Chem Eng J. 2014; 255: 585-592.
32. Huang J, Yi S, Zheng C, Lo IM. Persulfate activation by natural zeolite supported nanoscale zero-valent iron for trichloroethylene degradation in groundwater. Science Total Environ. 2019; 684: 351-359.
33. McGuire ME, Schaefer C, Richards T, Backe WJ, Field JA, Houtz E, et al. Evidence of remediation-induced alteration of subsurface poly- and perfluoroalkyl substance distribution at a former firefighter training area. Environ Sci Technol. 2014; 48: 6644-6652.
34. Harding-Marjanovic KC, Yi S, Weathers TS, Sharp JO, Sedlak DL, Alvarez-Cohen L. Effects of aqueous film-forming foams (AFFFs) on trichloroethene (TCE) dechlorination by a dehalococcoides mccartyi-containing microbial community. Environ Sci Technol. 2016; 50: 3352-3361.
35. Carter KE, Farrell J. Electrochemical oxidation of trichloroethylene using boron-doped diamond film electrodes. Environ Sci Technol. 2009; 43: 8350-8354.
36. Chen G, Betterton EA, Arnold RG, Ela WP. Electrolytic reduction of trichloroethylene and chloroform at a Pt- or Pd-coated ceramic cathode. J Appl Electrochem. 2003; 33: 161-169.
37. U.S. EPA. Method 551.1: Determination of chlorination disinfection byproducts, chlorinated solvents, and halogen pesticides/herbicides in drinking water by liquid extraction and gas chromatography with electron-capture detection. Cincinnati, OH: USEPA; 1995.
38. Skoog DA, Holler FJ, Crouch SR. Principles of instrumental analysis. USA: Cengage Learning; 2017.
39. Garcia-Costa AL, Savall A, Zazo JA, Casas JA, Serrano KG. On the role of the cathode for the electro-oxidation of perfluorooctanoic acid. Catalysts. 2020; 10: 902.
40. Cañizares P, García-Gómez J, Fernández de Marcos I, Rodrigo MA, Lobato J. Measurement of mass-transfer coefficients by an electrochemical technique. J Chem Educ. 2006; 83: 1204.

41. Pereira LA, Martins LF, Ascenso JR, Morgado P, Ramalho JP, Filipe EJ. Diffusion coefficients of fluorinated surfactants in water: Experimental results and prediction by computer simulation. J Chem Eng Data. 2014; 59: 3151-3159.
42. Legrand J, Dumont E, Comiti J, Fayolle F. Diffusion coefficients of ferricyanide ions in polymeric solutions-Comparison of different experimental methods. Electrochim Acta. 2000; 45: 1791-1803.
43. Rossi F, Cucciniello R, Intiso A, Proto A, Motta O, Marchettini N. Determination of the trichloroethylene diffusion coefficient in water. AIChE J. 2015; 61: 3511-3515.
44. Mostafa E, Reinsberg P, Garcia-Segura S, Baltruschat H. Chlorine species evolution during electrochlorination on boron-doped diamond anodes: In-situ electrogeneration of Cl_2, Cl_2O and ClO_2. Electrochim Acta. 2018; 281: 831-840.
45. Donaghue A, Chaplin BP. Effect of select organic compounds on perchlorate formation at boron-doped diamond film anodes. Environ Sci Technol. 2013; 47: 12391-12399.
46. Lin Z, Yao W, Wang Y, Yu G, Deng S, Huang J, et al. Perchlorate formation during the electro-peroxone treatment of chloride-containing water: Effects of operational parameters and control strategies. Water Res. 2016; 88: 691-702.
47. Jung YJ, Baek KW, Oh BS, Kang JW. An investigation of the formation of chlorate and perchlorate during electrolysis using Pt/Ti electrodes: The effects of pH and reactive oxygen species and the results of kinetic studies. Water Res. 2010; 44: 5345-5355.
48. Bergmann ME, Koparal AS, Iourtchouk T. Electrochemical advanced oxidation processes, formation of halogenate and perhalogenate species: A critical review. Crit Rev Environ Sci Technol. 2014; 44: 348-390.
49. Urbansky ET. Perchlorate as an environmental contaminant. Environ Sci Pollut Res Int. 2002; 9: 187-192.